IOPscience iopscience.iop.org

Home Search Collections Journals About Contact us My IOPscience

Adsorbate-induced reconstruction of surfaces: An atomistic alternative to microscopic faceting?

This article has been downloaded from IOPscience. Please scroll down to see the full text article.

1994 J. Phys.: Condens. Matter 6 6067

(http://iopscience.iop.org/0953-8984/6/31/007)

View the table of contents for this issue, or go to the journal homepage for more

Download details:
IP Address: 171.66.16.147
The article was downloaded on 12/05/2010 at 19:04

Please note that terms and conditions apply.

J. Phys.: Condens. Matter 6 (1994) 6067–6094. Printed in the UK

REVIEW ARTICLE

Adsorbate-induced reconstruction of surfaces: an atomistic alternative to microscopic faceting?

D P Woodruff
Physics Department, University of Warwick, Coventry CV4 7AL, UK

Received 25 February 1994, in final form 21 April 1994

Abstract. There is increasing evidence that there exists a class of adsorbate-induced reconstructions of metal surfaces in which the outermost substrate layer (or layers) and the adsorbed species adopt an almost identical geometry on surfaces of several different orientations of the same substrate; on one orientation this involves little or no substrate distortion, but on the others, major reconstruction is required. There is also evidence that the adsorption structure on the unreconstructed orientation surface may have a particularly low surface free energy. This type of reconstruction therefore appears to offer an atomistic alternative to the more microscopic phenomenon of adsorbate-induced faceting. By reviewing the existing structural information concerning the adsorbate structures of S on Ni, Cu and Pt, C and N on Ni and Cu and O on Cu, the evidence for this idea, and for some complementary patterns of adsorbate-induced reconstruction, are discussed. These data on the long-range-ordered phases on the (100), (111) and (110) faces of these materials are compared with the limited data available on the influence of the adsorbates on the anisotropy of the surface free energy, or γ-plot.

1. Introduction

Whilst the phenomenon of adsorbate-induced reconstruction of well characterized single-crystal surfaces is not a newly recognized effect, recent work has identified an increasing number of examples and is leading to the conclusion that it is far more widespread than had previously been thought [1, 2]. To some extent this changed perception is a result of overcoming early preconceptions, and of increasing confidence in structural methods. In particular, many early quantitative structural studies of surfaces did not consider the *possibility* that substrate reconstruction might be involved, whilst in others 'simple' cases were sought deliberately to test the methods. Adsorbate-induced reconstruction can take a variety of forms [1, 2]. At the lowest level of surface modification, adsorbates often influence the subtle changes in atomic layer spacings that occur close to the surface of a clean substrate. At the other end of the spectrum of surface disruption, multilayer 'surface' compound formation can occur (e.g. surface halide formation [3]). Surface reaction with an ambient gas (or liquid) can also give rise to compound formation in which the layer thickness is restricted not by the thermodynamics, but by the kinetic flow of reactive ingredients to the reacting interface.

Here we concentrate on adsorbate-induced reconstructions that involve major disruption of at least one outermost layer of the substrate, typically changing the substrate species atomic density in this layer, but that fall short of bulk (multilayer) compound formation. A particular object of this paper is to survey the evidence suggesting that one class of adsorbate-induced substrate reconstructions may have much in common with, but provide an atomistic-scale alternative to, the more microscopic phenomenon of adsorbate-induced

0953-8984/94/316067+28$19.50 © 1994 IOP Publishing Ltd

faceting of surfaces. These reconstructions are those in which a surface phase is formed, comprising both adsorbate and substrate layer(s), which but for slight distortions is identical on several different crystal faces of the substrate material. There is now considerable qualitative, and some quantitative, evidence for the existence of quite a number of these structures. One such example concerns the adsorption of S on Ni surfaces. It is well known that on Ni(100) S forms a half-monolayer c(2 × 2) chemisorption structure in which the S atoms occupy fourfold-coordinated hollow sites on an essentially unreconstructed (although possibly distorted [4]) substrate (see figure 1(a)). However, at least one structure formed by S adsorption on Ni(111) appears to result from a reordering of top-layer Ni atoms to a (distorted) Ni(100)-like square mesh in which S atoms also occupy the hollow sites [5–11] (see figure 1(b)). In effect, the topmost layer of the Ni(111) is therefore the same as in Ni(100)c(2 × 2)–S. It is perhaps a matter of semantics as to whether this is described as a 'surface compound' or a chemisorption structure, but by contrasting this behaviour with that of S on Cu surfaces (see section 3.1.2) we believe a clear distinction can be drawn.

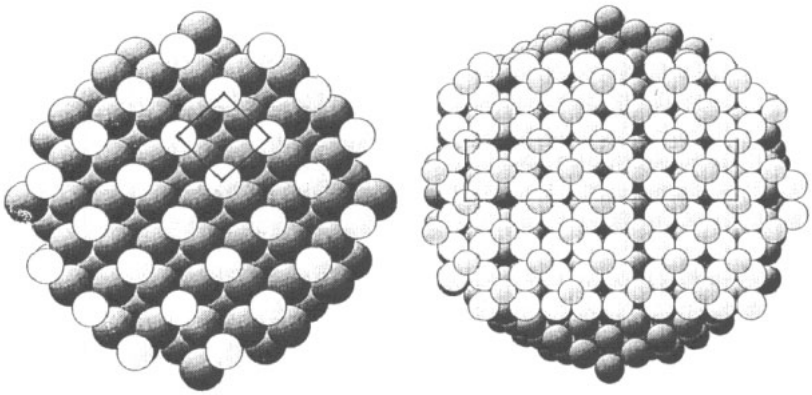

Figure 1. The top views of models of the (a) Ni(100)c(2 × 2)–S and (b) Ni(111)(5$\sqrt{3}$ × 2)rect.–S structures. In each case the larger shaded balls represent the Ni atoms and the smaller shaded balls represent the S atoms. In the case of the Ni(111)(5$\sqrt{3}$ × 2)rect. phase, for which the pseudo-(100) reconstruction model is shown, the outermost reconstructed Ni atoms are shown lighter than the substrate atoms, and the edge of the cluster is shown devoid of the Ni and S overlayer. The unit meshes are superimposed on each model.

Our object in this paper is to compare and contrast this behaviour with the far longer recognized, and more macroscopic, form of adsorbate-induced surface reconstruction, namely the phenomenon of faceting. Any structural transformation is, of course, driven by energy lowering, but faceting on macroscopic surfaces does require large-scale atom transport. Reconstruction of the top one or two monolayers of a substrate offers a potential route to surface-energy lowering that was not considered in earlier (pairwise bonding) theories of surface stability, and it is interesting to consider its potential generality, and indeed to try to establish whether such structures are true minimum-energy phases or whether they are simply metastable.

In order to set this idea in perspective, a small range of adsorption structures is surveyed, which provides examples of essentially three different classes of reconstruction. One of

these involves the particularly stable chemisorption phases described above. The other two involve structural phases that relate closely to elements of stable bulk compound structures: in the case of S on Cu, for example, the reconstructed surface phases appear to be based on the full three-dimensional character of the bulk compound, but for the case of O on Cu the key structural element common to both the surface reconstructions and many bulk compounds is that of one-dimensional chains.

The organization of the material is as follows. In section 2, the established background to surface free-energy anisotropy and its relationship to the equilibrium shape of small particles is briefly reviewed. A specific example of Pt surfaces and effect of adsorption of S on them is included. In addition, the development of this background to the stability of macroscopic surfaces to faceting transitions is described, and some of the key questions concerning the role of alternative surface reconstructions are introduced. This is followed in section 3 by reviews of a series of case studies of specific adsorption systems, choosing examples in which there is limited information available on both chemisorption-induced surface reconstructions and on grosser structural changes (faceting). The quality of the structural information in these examples varies considerably, from speculation based on the observed surface periodicity alone to full quantitative structure determinations. Nevertheless, by looking at a small range of structures, clear patterns can be discerned in this fragmentary data base. The set of model systems chosen is certainly not exhaustive, but is rather chosen to be illustrative. In section 4 some of the general features, including some of the problems of interpretation, are discussed.

2. Surface free energy and structural modifications

2.1. The γ-plot and the equilibrium shape of small particles

In equilibrium, the shape of a solid particle is determined by the criterion of minimizing the total surface free energy. If the surface (Gibbs) free energy, γ, were independent of orientation, as in a liquid, this would clearly result in a spherical shape. In the case of a solid, which has an anisotropic γ, this leads to a shape in which orientations of low surface free energy are more prominent, despite the increase in total surface area that results from this shape. Formally, the requirement is to minimize the integral $\int \gamma(n)\,\mathrm{d}S$ over the whole body, where $\gamma(n)$ is the surface free energy as a function of the direction of the surface unit normal n and $\mathrm{d}S$ is an element of surface area. The graphical solution to this problem is known as the Wulff construction and was first proposed in 1901 [12]. Starting from a plot of the surface free energy $\gamma(n)$ in polar coordinates (the γ-plot) one constructs a series of planes perpendicular to the radius vectors at the point at which these intersect the γ-plot. The inner envelope of these planes gives the shape of the minimum-surface-energy body.

A substantial body of older experimental literature exists concerning the γ-plot and equilibrium shapes. One route to determining portions of the γ-plot [13] is to measure the equilibrium shape of small particles. Typically, these measurements have been made at high temperature (say 80–90% of the absolute melting point) and with small particles (micrometre scale or, using electron microscopy, much smaller) in order that the substantial mass transport needed to establish the equilibrium shape can occur. Clearly the existence of singular minima (cusps) in the γ-plot at low-Miller-index faces leads to facets at these orientations and also to gaps in the experimental γ-plot near these orientations. Portions of the γ-plot can also be obtained by various kinds of intersecting-boundary method [14] in which the angles of intersection (in equilibrium) can be used to determine the balance of surface tension forces. An added complication in such studies is the role of the 'torque

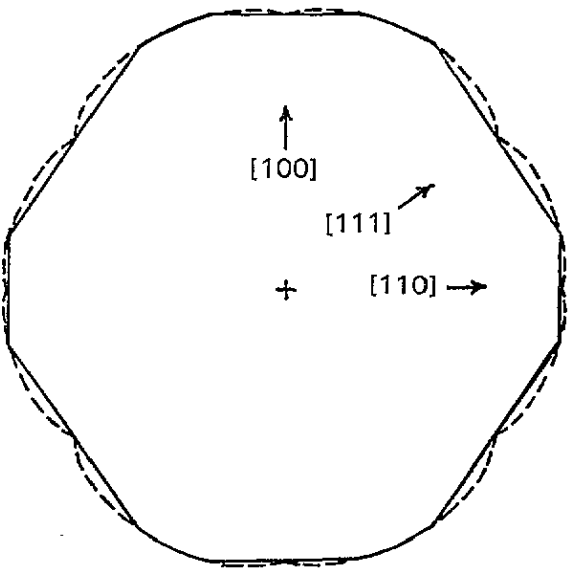

Figure 2. The experimental γ-plot for Pt (dashed line) and the implied equilibrium shape (full line) (after Mykura and McLean [14, 15]).

terms', forces representing the desire of the surface to move to an orientation of lower surface free energy as determined by the local gradients of the γ-plot.

As an example of experimental measurements of γ-plots we describe briefly some results for clean and adsorbate-covered Pt. In figure 2, an experimental γ-plot is shown for Pt (based on measurements at 1500 °C) together with the inferred equilibrium particle shape [14, 15]. These data were obtained through studies of twin boundary grooves on macroscopic foils by optical (interference) microscopy, a method requiring atomic movements over distances of many micrometres; in such a situation equilibration can only be achieved in reasonable times at high temperatures. The results show the deepest cusp in the γ-plot for the (111) orientation, with a shallow cusp at (100). The observation of the lowest free energy for the close-packed (111) surface is consistent with expectations from simple pairwise interaction models.

Direct measurements by electron microscopy of the equilibrium shape of very small Pt particles ($\sim$ 100 Å) in the presence of chemisorbed S [16], on the other hand, show the particles to be cubic, with (100) faces exposed, clearly indicating that under these circumstances the deepest cusp in the γ-plot occurs for the (100) orientation. These experiments involved equilibration at 500 °C in a 100 ppm partial pressure of H_2S in H_2, the much lower temperature being adequate for rapid equilibration of such small particles. It is therefore tempting to interpret this large difference in anisotropy as due entirely to the S adsorption. In comparing the results of these two experiments we should recognize, however, that there is a rather substantial difference between the temperatures at which they were performed, so that not all the differences are associated with the S adsorption. Elevated temperatures do affect the γ-plot and the associated equilibrium shape via disordering, which reduces the depth of the cusps, and also, at least on high-Miller-index surfaces, by roughening transitions, which can entirely remove such cusps [12, 17]. For this reason, the equilibrium shape of clean Pt at lower temperature would probably show additional, or larger, facets than those implied by the data of figure 2. Such effects can, of course,

be related to the surface entropy, but there have been very few examples of attempts to measure this quantity for any surfaces.

In fact similar electron-microscopy studies of small Pt particles grown or annealed in H_2, N_2 and air at 500 °C indicate that the true clean-surface γ-plot at this lower temperature may also shown the deepest cusps at (100) [18]. In particular, in an H_2 atmosphere essentially cubic particles were seen, albeit with significant (110) corner facets; the H_2 atmosphere is commonly used in such studies to prevent the build-up of contaminant adsorbates, as this gas removes surface C and O at elevated temperatures but should not itself have substantial residence time on the surface [18–20]. This particular set of measurements seemed to indicate that adsorption of contaminants greatly *reduces* the magnitude of the anisotropy of the γ-plot, but this is clearly not the case for the S chemisorption situation. Despite the ambiguity in the exact details of the clean Pt surface γ-plot [21], which may therefore differ significantly from that shown in figure 2, at least at lower ($\sim$ 500 °C) temperatures, it seems clear that on the S-covered surface the (100) cusp corresponds to by far the deepest cusp, as *only* this orientation is present on the (cubic) equilibrium-shape particles. Not only do these results show that adsorption can modify the γ-plot, but they also indicate that the chemisorption structure formed by S on Pt(100) has a particularly low surface energy. The electron microscopy results actually show that the (100) facets of the small particles show a simple c(2 × 2)–S chemisorption structure, which is not believed to involve any substrate reconstruction [23].

2.2. *Faceting and reconstruction*

Whilst the equilibrium shape of small particles is readily related to the form of the anisotropy of the surface free energy, most modern surface-science experiments are conducted on large ($\sim$ 1 cm) flat thin crystals and clearly cannot be expected to reach their true equilibrium shapes in any available experimental time scale. Under certain circumstances, however, a flat surface can lower its energy by developing a 'hill-and-valley' structure, typically involving faceting. For example, a vicinal surface close to a low-index face having a particularly low surface free energy may break up into large regions of the low-index facet connected by other suitable faces; as in the case of the equilibrium shape itself, a decrease in the total surface free energy can still be associated with an increase in the total surface area. The criterion for this instability has been investigated by Herring [25], who showed that any surface orientation not represented on the equilibrium shape of a small particle (as given by the Wulff construction) is unstable to this kind of transition. This means that the equilibrium shape can have a real relevance for studies of macroscopic flat single-crystal surfaces as commonly used in surface science, despite the fact that such crystals clearly cannot adopt completely this ideal equilibrium shape.

In practice, faceting of single-crystal surfaces is not very commonly observed in surface-science studies. There are at least two possible reasons for this. The first is that most such studies are conducted on low-Miller-index surfaces, and whilst chemisorption may lead to a significant increase in the anisotropy of the γ-plot, cusps are probably very often retained at these low-index orientations, which then remain on the equilibrium shape. On the other hand, the results described in the previous section for the Pt/S system would imply that faceting should occur on Pt(111) and (110) surfaces in the presence of adsorbed S, because neither of these orientations appear on the equilibrium shape. On the (111) face a stable chemisorption structure involving no significant reconstruction is seen, albeit at the lower coverage of 0.33 ML [26], although a more complex structure is seen at higher coverage [27–29]. On Pt(110) adsorbed S gives rise to a range of lange-range-ordered structures [27–30] for which detailed structural analyses are not available. The possibility that some

form of substrate reconstruction could be involved on both surfaces will be reconsidered in detail in subsection 3.1.3. In neither case, however, do there appear to be reports of observations of faceting.

The second reason for the relatively rare observation of faceting, however, may be that the surfaces studied are not generally allowed to adopt their equilibrium morphology. For several years there were strongly voiced objections to reconstruction models of surfaces (e.g. missing-row models of FCC (110) metal surfaces) based on the idea that the mass transport needed to form the reconstructions could not occur at the temperature at which these reconstructive transitions occur (which can be as low as room temperature). We now know, from STM results in particular (e.g. [32]), that this mass transport involving only atoms of the surface layer, and using step edges as sources or sinks of atoms, can occur quite easily. Faceting, however, requires mass transport on a far more massive scale. In particular, if one low-index face facets to another facet angles in the range 35–45° (or higher) are required, so the depth of the facets (and of the mass transport required) must be comparable to the lateral dimensions, which for diffraction techniques, at least, need to be of the order of 100 Å to be observed. Despite this, there are reports of adsorbate-induced faceting being observed on macroscopic flat single-crystal surfaces at temperatures as low as 133 K [33]. More generally, however, it is entirely possible that some apparently stable chemisorption structures studied in surface science are only metastable, and that a faceted surface represents the true equilibrium state.

In this context of the stability or metastability of chemisorption structures, we wish to highlight the class of adsorbate-induced surface reconstructions in which one low-index face adopts a surface layer in which atoms of the substrate species occupy a mesh very similar to that of another (unreconstructed) low-index face. The examples we shall consider here all involve square (100)-like layers forming on (111) and (110) FCC substrate surfaces, such as the Ni(111)/S example mentioned in section 1. Of course, reconstruction only occurs because the free energy of the new structure is lower than that of a simple unreconstructed chemisorption structure on this face. If the outermost substrate layer(s) are involved in significant changes in position parallel to the surface (and in surface-density changes), the free energy can be regarded as composed of two terms, one associated with the interface between the vacuum and the reconstructed layer, and one (purely derived from strain energy) between the substrate and the reconstructed layer. If the reconstructed layer is identical in structure to that of the low-index face it reproduces, it is clear from this separation that the total surface free energy of this reconstructed face must be larger than that of the unreconstructed face whose structure it mimics (which has no associated substrate-reconstructed overlayer strain energy). However, the reconstructed overlayer is invariably a slightly distorted version of the unreconstructed face, so the vacuum–solid interfacial free energy *could* be lower on the reconstructed face. On the other hand, this distortion is brought about to relieve the interfacial strain, so it seems likely that the reconstructed face will normally have a higher surface free energy than the unreconstructed face it mimics.

This raises an interesting question: is the reconstruction a true equilibrium state, or is it simply metastable, a faceted surface having an even lower free energy? Alternatively, does the reconstruction lower the surface free energy sufficiently that the surface becomes stable to faceting to a hill-and-valley structure, only part of which has a lower specific surface free energy? (In this case it is likely that the pseudo-(100) reconstructed face will itself correspond to a cusp minimum on the γ-plot, so we would expect nearby vicinals to facet to this reconstructed low-index face). Eventually, if the (100)-faceted surface does have the lower energy, what is the energy barrier preventing the transformation? The most obvious answer to this would be the extra edge energy needed in the early stages of the transition

when the facets are very small—this is equivalent to the usual nucleation problem in two- and three-dimensional growth.

3. Adsorbate-induced reconstruction: case studies

3.1. S adsorption structures

As examples of different kinds of behaviour we consider three different representative metals, Ni, Cu and Pt. Note that most of the S adsorption structures discussed here were formed via the interaction of H_2S with the metal surface, although a few studies used molecular beams of S. However, as we are concerned here with the stability of the structural phases and not the reaction chemistry, these details will not be discussed extensively.

3.1.1. Ni/S systems. The case of Ni(111)/S has already been mentioned in section 1, and represents one of the very first cases of a proposal, by the BP research group [5, 6], of surface reconstruction to generate a surface phase essentially identical to that of a simple unreconstructed chemisorption structure of another face ((100)). S adsorption structures on Ni surfaces have been studied extensively, typically by H_2S dissociation over the appropriate surface, but also by dissociation of thiols and other compounds, and by segregation of dissolved S to the surface. In all cases a variety of surface temperatures for adsorption and annealing have been investigated. A summary of the various long-range-ordered structures seen on the three low-index faces of Ni in the presence of adsorbed S is given in table 1. In general the Wood notation [34] is used for these phases, but where possible ambiguities exist, the matrix notation [35] is also shown. Such ambiguity arises when the included angle of the new surface mesh differs from that of the substrate mesh. In particular, some rectangular mesh structures are seen on the (111) face, and in these cases 'rect.' is added to the modified Wood notation to show the included angle is 90°. In the case of the matrix notation for the (111) surface, the matrix is based on the use of primitive translation vectors separated by 60°, as seems to be most commonly used in the literature, rather than the 120° used in formal definitions of the two-dimensional Bravais net. Approximate S surface coverages are also given in monolayers (ML) defined as one adsorbate atom per substrate atom in a layer parallel to the surface. Because these coverage units differ for the three orientations considered, coverages are also expressed in common units of (100) monolayers. The coverages shown are the nominal saturation coverages, typically based on the assumed or proven structure, but generally supported (to lower precision) by quantitative experimental measurements. In most of the systems described in this paper, such coverage calibrations have been by Auger electron spectroscopy or XPS; in the particular case of S on Ni, most of these measurements (by the Paris group of Oudar and coworkers [28–31, 49, 56] were calibrated using radioactive S species.

On the (100) surface only the simple overlayer mesh structures ($p(2\times2)$ and $c(2\times2)$) are formed, and quantitative structural analyses by LEED, SEXAFS and photoelectron diffraction (e.g. [36–42]) are all in general agreement that S adsorbs into the maximally coordinated (fourfold) hollow sites with no significant substrate reconstruction (although it seems possible that there are small (less than about 0.1 Å) distortions of second-layer substrate-atom locations). Similar simple overlayer structures involving the maximally coordinated hollow site have been found to correspond to the Ni(111) (2×2)–S, Ni(111) $(\sqrt{3}\times\sqrt{3})$R30°–S and Ni(110)c(2×2)–S structures [7, 43–48]. On these surfaces, however, there is a range of other structures seen, including the larger mesh structures on Ni(111), which are thought

Table 1. Long-range-ordered structures formed by S adsorption on Ni surfaces.

	Phase		Coverage	
Surface	Wood	Matrix	(ML)	((100)-equivalent ML)
Ni(100)	p(2 × 2)		0.25	0.25
	c(2 × 2)		0.50	0.50
Ni(111)	(2 × 2)		0.25	0.29
	(√3 × √3)R30°		0.33	0.38
	c(5√3 × 9)rect.	$\begin{vmatrix} 7 & -2 \\ -2 & 7 \end{vmatrix}$	0.22	0.26
	(5√3 × 2)rect.	$\begin{vmatrix} 2 & 0 \\ -5 & 10 \end{vmatrix}$	0.40	0.46
	(8√3 × 2)rect.	$\begin{vmatrix} 2 & 0 \\ -8 & 16 \end{vmatrix}$	0.41	0.47
Ni(110)	c(2 × 2)		0.50	0.35
	p(5 × 2)		0.60	0.42
	c(8 × 2)		0.63	0.44
	p(3 × 2)		0.67	0.47
	p(4 × 1)		0.75	0.53

likely to derive from coincidence lattice structures, which might involve reconstruction (e.g. (5√3 × 2) rect.).

The complexity of these large unit mesh structures on Ni(111) makes it difficult to obtain unique quantitative structural assignments. Edmonds *et al* [6], however, have shown that the three structures they observe after higher-temperature treatments or at higher chemisorption coverages can all be accounted for geometrically by slightly distorted Ni(100) overlayer structures. In particular, a (111)c(5√3 × 9)rect. structure (correctly identified but described ambiguously as (√39 × √39)R16° in terms of an oblique mesh in the original work), formed by heating the (111)(2 × 2) phase, can be associated with a Ni(110)p(2 × 2)–S overlayer, whilst the two other phases, normally referred to as (111)(5√3 × 2)rect. and (111)(8√3 × 2)rect., can be accounted for by outmost layers being modifications of Ni(100)c(2 × 2)–S overlayers. Somewhat similar models were also proposed in the early work of Perdereau and Oudar [49].

The Ni(111)(5√3 × 2)rect.–S phase has been the subject of several more recent experiments. In particular, two independent SEXAFS studies [7, 8] have given strong quantitative support to this pseudo-(100) reconstruction model (figure 1(b)). Recent STM images, which show 'troughs' in this structure, have been interpreted as indicating a quite different, missing-row, model [9], but this alternative model is inconsistent with the SEXAFS results [10], and it has been suggested that the pseudo-(100) reconstruction model can be reconciled with the STM images by including, for example, the effect of corrugation in the reconstructed overlayer [10, 11]. This large surface mesh structure is too complex for a full quantitative structure analysis by these methods, but a very recent surface x-ray diffraction study [148], which is able to obtain a far more complete picture, confirms the essential local square geometry of the pseudo-(100) reconstruction, but finds quite a large distortion similar to that seen in the Ni(100)(2 × 2)–C phase discussed below in subsection 3.2. In addition to this work on the (5√3 × 2)rect. phase, semiquantitative LEED results from c(5√3 × 9)rect. structures formed by C and N adsorption on Ni(111) (also described in subsection 3.2) support the pseudo-(100) reconstruction model for these phases and thus suggest that a similar model may be appropriate to this structure formed by S adsorption. This all lends credence to the complete set of proposed structures based

on modifications of this model. Note that under more extreme S exposure conditions Edmonds *et al* have observed further LEED patterns consistent with true (bulk-like) nickel sulphide overlayers forming, distinguishing the reconstructed chemisorption structures from true compound formation.

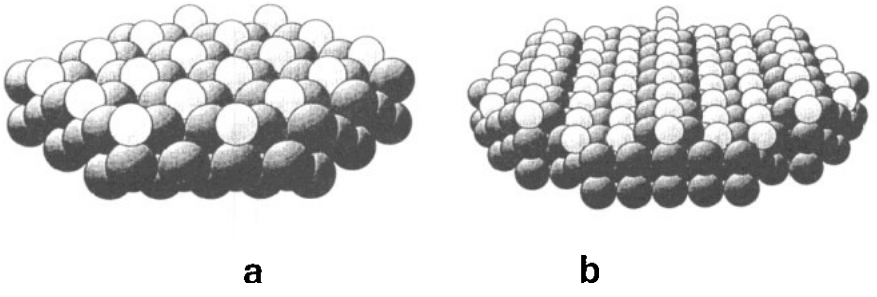

Figure 3. Perspective views of models of the (a) Ni(110)c(2 × 2–S and (b) Ni(110)(4 × 1)–S structures, looking along the close-packed ⟨110⟩ azimuth. In each case the larger shaded balls represent the Ni atoms and the smaller shaded balls represent the S atoms.

On the Ni(110) surface the simple c(2 × 2) overlayer structure (figure 3(a)) is replaced at higher coverages by a series of structures associated with splitting of LEED beams and apparent compression of the S submesh along the ⟨110⟩ surface direction, the final saturation structure at room temperature being the p(3 × 2) phase [49]. The p(4 × 1) structure is only formed after exposure at elevated temperatures. Recent STM studies of these structures reveal that the room-temperature phases up to p(3 × 2) do not involve any apparent mass transport of Ni atoms and must therefore be simple overlayers rather than reconstructed phases [50, 51]. By contrast, the p(4 × 1) does appear to involve such reconstruction, and indeed a combination of STM [52] and surface x-ray diffraction [53] has provided an explicit model for this structure. This structure (figure 3(b)) has an outermost layer comprising 0.50 ML of Ni atoms, with S adsorbed in the hollow sites on the double rows that form the outermost layer, but additional S is adsorbed on the lower layer in sites that are remarked [54] to be very similar to those on Ni(100); in effect, the reconstruction provides microscopic (100) facets on which the S atoms are adsorbed. Thus, although this structure is certainly not a simple pseudo-(100) reconstruction, as proposed for the high-coverage (111)-face phases, the local structure after reconstruction has much in common with that on Ni(100).

One further piece of evidence indicating an exceptional stability for the Ni(100)c(2×2)–S surface structure comes from results on S adsorption on NiO(100) surfaces, for which there is evidence from both qualitative LEED and quantitative SEXAFS studies that a surface phase comprising a pseudo-Ni(100)c(2 × 2)–S structure occurs on this surface despite being *incommensurate* [54, 55].

On the (111) face the overlap in coverage range associated with the simple overlayer and reconstructed phases raises interesting problems concerning the true equilibrium structures and the role of elevated temperatures. The Ni(111)(2×2)–S and Ni($\sqrt{3}\times\sqrt{3}$)R30°–S phases correspond to nominal coverages of 0.25 ML and 0.33 ML (in (111) monolayers), but the reconstructed phases cover the range 0.22–0.41 ML, which straddles these values. The most obvious implication of the fact that the complex phases are formed by heating is that the simple S-overlayer structures are not the true minimum-energy structures. In this context it is interesting that there are relatively few reports of the ($\sqrt{3}$ × $\sqrt{3}$) phase being seen, suggesting its 'stability' range of coverage and temperature may be narrow.

In contrast to these extensive studies of the long-range-ordered phases formed on the three low-index faces, there do not appear to have been any detailed direct surface free-energy measurements made on this system, nor studies of equilibrium shapes of small particles or faceting. In fact, Edmonds *et al* [6] did report the observation of 'weak facets' on both Ni(100) and (111) after annealing at the highest temperatures (1200 K) following S treatments. They give no details of the nature of these facets, but it is certainly possible that at such elevated temperatures in UHV, they may well result from selective evaporation rather than from an equilibrium-shape-driven phenomenon. Perdereau and Oudar [49] also comment on faceting of the nominal Ni(111) face, apparently even at room temperature, for slight misorientations of the surface, but give no details of this behaviour.

Table 2. Long-range-ordered structures formed by S adsorption on Cu surfaces.

	Phase		Coverage	
Surface	Wood	Matrix	(ML)	((100)-equivalent ML)
Cu(100)	p(2 × 2)		0.25	0.25
	(√17 × √17)R14°	$\begin{vmatrix} 4 & -1 \\ 1 & 4 \end{vmatrix}$	0.47	0.47
Cu(111)	(2 × 2)		0.25	0.29
	(√3 × √3)R30°		0.33	0.38
	(√7 × √7)R19°		0.43	0.50
Cu(110)	c(2 × 2)		0.50	0.35
	compression via p(5 × 2) and c(8 × 2) to p(3 × 2)		0.67	0.47

3.1.2. Cu/S systems. Similar studies of S chemisorption structures on Cu surfaces [56], summarized in table 2 using the same format as for table 1, reveal a somewhat different picture. On all three low-index surfaces there is evidence for simple small-unit-mesh overlayer structures as well as for more complex higher-coverage phases which are thought to involve substrate reconstruction; it has been suggested, and this suggestion has been supported by rather limited quantitative investigations, that these reconstructed faces all adopt structures similar to those of bulk sulphides.

Of the three simple (proposed overlayer) phases, (100)p(2 × 2), (111)(√3 × √3)R30° and (110)c(2 × 2), only the Cu(100)p(2 × 2)–S phase has been studied extensively by quantitative methods, and there is a clear consensus that a simple S overlayer with the S atoms occupying the hollow sites is involved [57–67] (as for Ni(100)p(2 × 2)–S). Although there is no evidence for true substrate reconstruction in this phase, the more recent and more detailed analyses [60, 64–67] do indicate that the four Cu atoms around the adsorbed S atom move away from the hollow parallel to the surface by a small amount (0.04 Å) to 'open up' the hollow. It is also interesting to note that, in contrast to the situation for Ni(100)/S, no c(2 × 2)–S phase is formed on Cu(100). The extensive literature on the Cu(100)p(2 × 2)–S phase bears witness to the stability and ease of preparation of this phase; by contrast, the Cu(111)(√3 × √3)R30°–S phase is not always seen in studies of S adsorption on Cu(111) [68, 69], suggesting that it may have a narrow range of stability in temperature and coverage (like the Ni(111)(√3 × √3)R30°–S phase).

At higher coverages, (√17 × √17)R14° and (√7 × √7)R19° structures are formed on Cu(100) and Cu(111) respectively, and on Cu(110) there appears to be a range of structures

involving continuous 'compression' of the overlayer mesh along the ⟨100⟩ azimuth with increasing coverage, terminating in a (3 × 2) structure. In the original paper by Domange and Oudar [56] all of these structures were proposed to involve a mixed Cu/S overlayer having a geometry similar to that of different crystal planes of CuS_2.

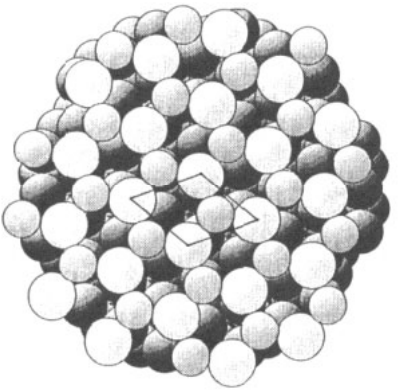

Figure 4. The top view of a model of the Cu(111)($\sqrt{7}\times\sqrt{7}$)R19°–S structure. The larger shaded balls represent the Cu atoms and the smaller shaded balls represent the S atoms. The outermost reconstructed Cu atoms in the 'surface sulphide' are shown lighter than the substrate atoms. The unit mesh is superimposed.

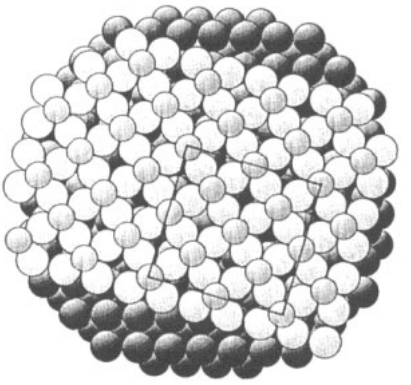

Figure 5. The top view of a model of the Cu(100)($\sqrt{17}\times\sqrt{17}$)R14°–S structure. The larger shaded balls represent the Cu atoms and the smaller shaded balls represent the S atoms. The outermost reconstructed layer Cu atoms are shown lighter than the substrate atoms, and the edge of the cluster is shown devoid of the Cu and S overlayer so that the registry can be seen. The unit mesh is superimposed.

On the (111) face the only quantitative structural investigation is a combined SEXAFS and standing x-ray wavefield absorption study of the Cu(111)($\sqrt{7}\times\sqrt{7}$)R19°–S phase, which concluded that the data were compatible with the sulphide model, and which provided some detailed structural parameter values (figure 4) [69]. STM studies [70] of the formation of this structure have confirmed that reconstruction is involved, and that the outermost layer comprises $\frac{3}{7}$ ML of Cu atoms and $\frac{3}{7}$ ML of S atoms, consistent with the preferred sulphide model. These STM studies also identified an additional transitional phase, $\left|\begin{smallmatrix}4 & 1\\ -1 & 4\end{smallmatrix}\right|$, which probably accounts for earlier 'complex' LEED patterns involving a coexistence of two surface phases; here the STM allows the periodicity of local domains to be isolated, but no specific model for the structure of this phase is currently available.

On the (110) face, the only quantitative study is the application of SEXAFS [71] to a 'diffuse c(2 × 2)' phase, and to a range of the higher-coverage' 'compression' phases. Somewhat surprisingly, this work concluded not only that the S occupies the hollow site in the c(2 × 2) phase, as might be expected, but that at the higher coverages the S–Cu bondlength and bond angles were unchanged. There are also rather interesting STM results [72] for these structures. In particular, they find that during the 'compression' range, there is significant Cu atom mass transport on the surface, indicating that sulphide (i.e. mixed Cu/S) surface phases may be involved in some of these structures, although the net transport in producing the intermediate p(5 × 2) phase was apparently zero, leading to the suggestion that this particular phase, at least, may involve only a S overlayer. Notice that the same unit mesh occurs on Ni(110) in the presence of S, but in this case no net Ni mass transport

is seen to be associated with its formation. In the STM study, the final highest-coverage structure was a c(8 × 2) phase; the p(3 × 2) was not observed (in common with a more recent LEED study [73]).

Although there is no quantitative study of the higher-coverage S phase on Cu(100), it is interesting to note that the model suggested for this ($\sqrt{17} \times \sqrt{17}$)R14°–S structure [56] actually involves a square-mesh Cu overlayer with a submesh dimension of 3.72 Å and S atoms located in the hollow sites (figure 5). The fact that this mesh is slightly larger than that offered by the Cu(100) surface (3.61 Å), but is smaller than the Cu–Cu distance in CuS_2 (3.94 Å), is consistent with the slight hollow enlargement found in the LEED structure determination of the unreconstructed Cu(100)(2 × 2)–S structure, and with the absence of a Cu(100)c(2 × 2)–S phase. On the other hand, we note that the reconstructed sulphide overlayer in the Cu(11)($\sqrt{7} \times \sqrt{7}$)R19°–S structure has a hexagonal, rather than rectangular mesh (and is believed to be based on a hexagonal, rather than an almost square Cu submesh), so that the situation is quite different from that of Ni/S. The evidence therefore supports the view that the stable reconstructed high-coverage phases in the Cu/S system are essentially different 'single' layers of a common stable bulk compound, and not reconstruction to an especially stable chemisorption structure.

The difference between the Cu/S system and those of Ni/S and Pt/S is also highlighted by older studies of the effect of S adsorption on the γ-plot for Cu surfaces. In particular, Mykura [74] has used the 'torque-term method' [13, 14], which specifically investigates the gradient of the γ-plot around the cusps at the low-index faces, to study this problem at a temperature of 830 °C. While the (111) face of the clean surface is found to have the lowest surface free energy on clean Cu as expected for an FCC metal, similar measurements in a partial pressure of H_2S showed that the (110) developed the lowest surface free energy, and indeed the (100) surface actually acquired a *maximum* in the γ-plot, as witnessed by a negative gradient of γ with respect misorientation angle away from (100). Faceting of (110) vicinals to (110) was observed in the presence of S adsorbates, as might be expected from these results, although the anticipated break-up into a hill-and-valley structure of the (100) surface was not observed, possibly due to kinetic limitations. These results indicate that the Cu(100) surface, far from being the most stable structure in the presence of adsorbed S, is actually potentially unstable, and that the far more open-packed (110) face becomes the lowest-energy structure. Further support for this view is contained in more recent LEED studies of (110) vicinal surfaces, which were also found to facet to (110) at high coverages of S [73].

The structural results for the three low-index faces we have discussed above can only cast limited light on this finding of minimum surface free energy for the (110) face, although the fact that a continuous range of high-coverage S or sulphide structures is seen on this surface suggests that the corrugation, and thus perhaps the absolute value, of the overlayer-substrate interfacial energy is particularly low on this surface.

3.1.3. Pt/S systems. Finally, we return to a brief discussion of the structural data on the Pt/S system, for which we have clear evidence from the equilibrium-shape data [16] (as discussed in section 2) that the (100) face has a particularly low surface free energy in the presence of S. Indeed these data imply that the (110) and (111) faces should be unstable to faceting to (100) when S is adsorbed.

The long-range-ordered structures seen as a result of S adsorption on the low-index faces of Pt [26–31] are summarized in table 3. On the (100) face, (100)p(2 × 2) and (100)c(2 × 2) phases are seen, and while there are no quantitative analyses of these structures, their similarity to many other FCC(100) adsorption phases leads us to anticipate simple hollow-site overlayer structures. Of the three distinct long-range-order phases identified on the

Table 3. Long-range-ordered structures formed by S adsorption on Pt surfaces.

	Phase		Coverage	
Surface	Wood	Matrix	(ML)	((100)-equivalent ML)
Pt(100)	$p(2 \times 2)$		0.25	0.25
	$c(2 \times 2)$		0.50	0.50
Pt(111)	(2×2)		0.25	0.29
	$(\sqrt{3} \times \sqrt{3})R30°$		0.33	0.38
	$(\sqrt{3} \times 7)$rect.	$\begin{vmatrix} 4 & -1 \\ -1 & 2 \end{vmatrix}$	0.42	0.48
Pt(110)	$c(6 \times 2)$		0.33	0.23
	$p(2 \times 3)$		0.50	0.35
	$p(4 \times 3)$		0.67	0.47
	$c(2 \times 4)$		0.75	0.53
	$p(4 \times 4)$		0.81	0.57

(111) face ((2×2), $(\sqrt{3} \times \sqrt{3})R30°$ and $c(\sqrt{3} \times 7)$rect.), only the Pt(111)$(\sqrt{3} \times \sqrt{3})R30°$–S phase has been studied quantitatively (by LEED [26]) with the expected result that it is a simple overlayer structure involving S atoms in the hollow sites. We can reasonably expect that the Pt(111)(2×2)–S phase has a similar local geometry. In the formal report of the $c(\sqrt{3} \times 7)$ rect. phase [27], no attempt was made to propose a structural model, although the fact that the structure is lost on modest heating (to 300 °C) indicates it may be the *same phase interpreted by others as a 'compressed hexagonal' overlayer of S [28, 29]. The* surface coverage is essentially identical to that of the Pt(100)$c(2 \times 2)$–S structure, so it is tempting to consider the possibility that it involves an outermost-layer reconstruction to a pseudo-(100)$c(2 \times 2)$ structure. It is possible to devise such models, but fitting the surface mesh appears to require either a lower S coverage, or substantial compression (13%) of the Pt–Pt nearest-neighbour distance in one direction (which is compensated by a 17% expansion in the perpendicular direction). The ideally terminated Pt(100) surface is, of course, in a state of such high tensile surface stress that it undergoes a reconstruction to allow an increase in Pt atom surface density, but in the resulting close-packed overlayer the Pt–Pt nearest-neighbour distance is only 4% less than that of the bulk [22]. Moreover, the lack of thermal stability of the $c(\sqrt{3} \times 7)$rect. phase also contrasts with the behaviour of the S reconstructed overlayers found on Ni and Cu surfaces. On balance therefore, it seems unlikely that this structure does involve a pseudo-(100) reconstruction.

Finally, the adsorption of S on Pt(100) has been found to produce a succession of long-range structures at increasing S coverage—$c(6 \times 2)$, $p(2 \times 3)$, $p(4 \times 3)$, $c(2 \times 4)$, $p(4 \times 4)$; these structures have been interpreted in terms of regular arrays of S vacancies in an ideal S monolayer [31], although there is no quantitative structural analysis of any of them. As we shall see in the following section, Pt(110)(2×3) structures also form on Cu and Ni surfaces as a result of N adsorption, and there is hard evidence in these cases to support the idea that they are pseudo-(100) surface-phase reconstructions, so one might propose a similar structure for the Pt(110)(2×3)–S phase. Such a model, however, would then need to be reconciled, with appropriate modification, with all the other 'compression' phases, perhaps by considering similar regular vacancy and adatom modifications. In the absence of hard experimental evidence to distinguish such models, there seems little justification for pursuing this speculation.

3.1.4. Summary of S adsorption results. We may summarize the evidence concerning S

adsorption of the three principal low-index faces of Ni, Cu and Pt as follows:

(i) There are many examples of higher-coverage large-surface-mesh structures, which can be best understood in terms of commensurate overlayers of smaller submesh ('coincidence lattice structures'), for which models involving an overlayer comprising both S and metal atoms seem probable.

(ii) On Ni surfaces the absence of such complex structures on the (100) face, and the presence of several such structures on the (111) face, which can be accounted for in terms of a pseudo-(100) surface chemisorption structure, indicates that the (100)–S chemisorption structures are particularly stable and probably do form the basis of the (111) surface reconstruction phases. There is quantitative support for one of these models. Moreover, on Ni(110) the final highest-coverage phase does involve a kind of microfaceting to (100), with S atoms in the fourfold-coordinated hollow sites thus formed. Unfortunately, there are no complementary data on the role of S adsorption on the γ-plot to provide direct evidence of the relative surface free energies.

(iii) On Cu surfaces, there is evidence for high-coverage reconstruction on all three low-index faces, but the proposed mixed Cu/S overlayer phases do not have a common two-dimensional structure. Rather, they appear to correspond to different orientation slices through a common bulk sulphide phase. There is specific (SEXAFS and NISXW) quantitative support for the reconstruction of the (111) face. γ-plot data indicate the (110) surface has the lowest energy in the presence of S, and indeed appropriate vicinals are found to facet to this orientation.

(iv) On Pt surfaces the behaviour is far more similar to that of Ni in that on Pt(100) only simple overlayer structures are seen, whereas on the other two faces there are larger surface-mesh structures indicating reconstruction. However, the evidence for possible pseudo-(100)-face reconstructions on Pt surfaces is not very persuasive. Equilibrium-shape measurements show that the (100) face, with S adsorbed in the (2×2) and $c(2 \times 2)$ phases, is the lowest-energy structure. Indeed, the equilibrium-shape data indicate that both (111) and (110) surfaces should be unstable to faceting to (100) in the presence of adsorbed S, although this has not been observed in experiments on macroscopic crystal surfaces. The evidence therefore indicates that while the (100) chemisorption structures, as on Ni(100), have the lowest energy, it is not favourable to reconstruct the other low-index-orientation surfaces to this local structure, and faceting is the preferred route to energy lowering.

(v) The $(100)c(2 \times 2)$ chemsorption structure, which is thought to form the low-energy phase and the basis of most of the pseudo-(100) reconstruction structures on Ni, does not occur on Cu(100), which instead itself reconstructs at a fractionally lower S coverage (albeit to a similar *expanded* square pseudo-$(100)c(2 \times 2)$ structure).

3.2. C and N adsorption structures

We now consider the case of C and N adsorption phases on Ni and Cu surfaces. The Ni/C system is of especial interest not only because a rather subtle and extensively studied reconstruction is induced on the $(10\bar{0})$ face, but also because on the $(11\bar{1})$ face large-surface-mesh structures were seen and also interpreted in terms of pseudo-(100)-surface reconstructions in the early work of the BP group [5, 6]. Published information on the long-range-ordered structures seen on Ni surfaces resulting from chemisorbed C and N layers is summarized in table 4; this table does not include multi-layer graphitic overlayer structures, which effectively involve 'bulk' solid/solid interfaces. C overlayer structures have typically been prepared by the dissociation of small hydrocarbon molecules (e.g. acetylene) or CO on the surface. N structures have been formed either by the dissociation of N-containing

Table 4. Long-range-ordered structures formed by C and N adsorption on Ni and Cu surfaces.

	Phase		Coverage	
Surface	Wood	Matrix	(ML)	((100)-equivalent ML)
Ni(100)	p(2 × 2)–C		0.50	0.50
	p(2 × 2)–N		0.50	0.50
Ni(111)	c(5√3 × 9)rect.–C	$\begin{vmatrix} 7 & -2 \\ -2 & 7 \end{vmatrix}$	0.44	0.52
	c(5√3 × 9)rect.–N	$\begin{vmatrix} 7 & -2 \\ -2 & 7 \end{vmatrix}$	0.44	0.52
	'(2 × 6)'incomm.		~0.40	~0.46
Ni(110)	(2 × 1)–C		0.79?	0.56?
	(4 × 5)–C		0.79?	0.56?
	(2 × 3)–N		0.67	0.47
Cu(100)	c(2 × 2)–N		0.50	0.50
Cu(111)	'(1.48 × 1.44)rect.'–N		0.41	0.47
Cu(110)	(2 × 3)–N		0.67	0.47

molecules (mainly NH_3 but also acetonitrile) or by low-energy N ion bomabardment and annealing; molecular N_2 does not dissociate at Ni or Cu surfaces.

By far the greatest attention has been devoted to the Ni(100)p(2 × 2) phases formed by both C and N, because the C-induced structure was the first clear example of adsorbate-induced reconstruction on a metal surface [75], and there have been considerable efforts to try to understand the underlying mechanisms of the reconstruction. In both structures the adsorbate forms a c(2 × 2) mesh but the atoms penetrate the hollow sites (to adopt sites that are almost coplanar) and the nearest-neighbour Ni atoms move out and round the hollow in alternate clockwise and anti-clockwise movements to enlarge the penetrated hollow (figure 6). The mechanism is variously seen as associated with adsorbate interactions with the second-layer atoms directly below, or in the relief of the surface stress (the Ni atoms moving closer together in groups of four) [76–85]. The interrelationship of electronic and mechanical interactions is such that it is difficult to clearly identify a single cause, but the basic reconstruction is well established, with the initial qualitative LEED symmetry arguments [75] being supported by quantitative LEED, SEXAFS and photoelectron diffraction data [75, 86–90]. Notice that the nominal saturation coverage of these phases is 0.50 ML; the p(2 × 2) unit mesh is larger than the adsorbate submesh due to the Ni surface reconstruction, and contains two adsorbate atoms per unit mesh.

The nature of this reconstruction on the Ni(100) face is, of course, far more subtle that any of the S-induced reconstructions discussed in the previous section. In the present case, the Ni atom density in the surface is conserved, and the atomic displacements are relatively small. Indeed there is considerable evidence that the resulting chemisorption phase is extremely stable and of low energy. In particular, on Ni(111), the far more complex c(5√3 × 9)rect. phase, which is induced by adsorbed C, can be best understood in terms of a reconstruction of the outermost layer to a pseudo-(100)(2 × 2) structure. Notice that the c(5√3 × 9)rect. mesh is the same one as seen as a result of S adsorption on Ni(111) at a lower coverage and attributed to a reconstruction to a slightly distorted Ni(100)p(2 × 2)–S (0.25 ML) structure. The basic model is therefore the same for the C and S structures on Ni(111);

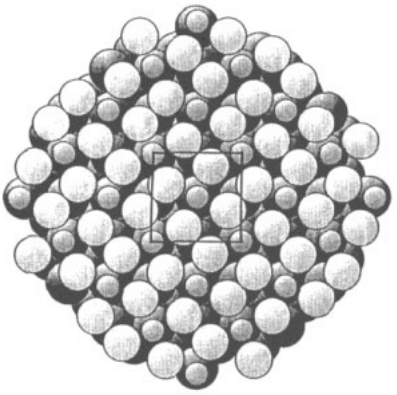

Figure 6. The top view of a model of the Ni(100)(2 × 2)–C p4g structure. The larger shaded balls represent the Ni atoms and the smaller shaded balls represent the S atoms. The outermost reconstructed layer Ni atoms are shown lighter (and with a slightly reduced radius). The unit mesh is superimposed.

the main difference is that the coverage is twice as large for C (twice as many fourfold-coordinated hollows occupied), while it is also possible that the C structure involves Ni atoms displacements parallel to the surface if the 'clock' reconstruction of the true Ni(100) structure of figure 6 persists on the (111) surface. This same surface mesh is also seen in the presence of adsorbed N produced via a variety of molecular decomposition routes [11, 91, 92]. Figure 7 shows the basic model involved in all of these structures: in figure 7(a) a layer of Ni adatoms on the nominal (100)(2 × 2) mesh is shown to demonstrate the basic match of periodicity of the pseudo-(100) overlayer and the (111) substrate. In figure 7(b), a complete pseudo-(100) NI layer is superimposed on the same substrate, together with 0.5 ML (in (100) units) of adsorbed atoms in the hollow sites. The overlayer submesh in this structure is effectively (100)c(2 × 2), but an S (2 × 2) overlayer structure can be obtained by simply removing alternate adsorbate atoms. Similarly, although the adsorbate coverage of figure 7(b) matches that of the C and N structures, no 'clock' distortion of the outermost layer is included. This can clearly be introduced with no change to the basic overlayer substrate registry.

Despite the appeal and consistency of these models, the large surface mesh makes it difficult to perform fully quantitative structural analyses by most conventional methods. The difficulty of such measurements is also hampered by the multiple overlayer domains, which result from the absence of the three-fold rotational symmetry of the substrate in the overlayer structure. Nevertheless, Gardin *et al* [11] have recently carried out measurements of LEED diffracted beam intensities from the C- and N-induced c($5\sqrt{3} \times 9$)rect. structures, specifically from single overlayer domains on selected areas of the sample, and compared these to the data from the (100)(2 × 2) structures produced by the same adsorbates. In particular, they measured intensities of beams occurring at scattering angles consistent with those of the (100)(2 × 2) structure, and find substantial similarity. On this basis they argue that the pseudo-(100) reconstruction model is strongly favoured. These results actually strongly imply another aspect of the structures which we have so far neglected: LEED intensities are determined by coherent interference of scattering from the outermost three or so atomic layers, so the model of figure 8(b) can only be reconciled with these LEED results if *several atomic layers of pseudo-(100) Ni structure* are involved, and not simply the outermost layer implied in our discussions so far. The attenuation of the (111)-related diffraction beams seen in these experiments is consistent with this idea. In this respect, we should note that the STM studies of the Ni(111)($5\sqrt{3} \times 2$)rect.–S structure do indicate that only the top Ni layer is reconstructed [9]. On the other hand, reconstructions of the clean faces of several rare-earth metals appear to involve similar multilayer reconstructions

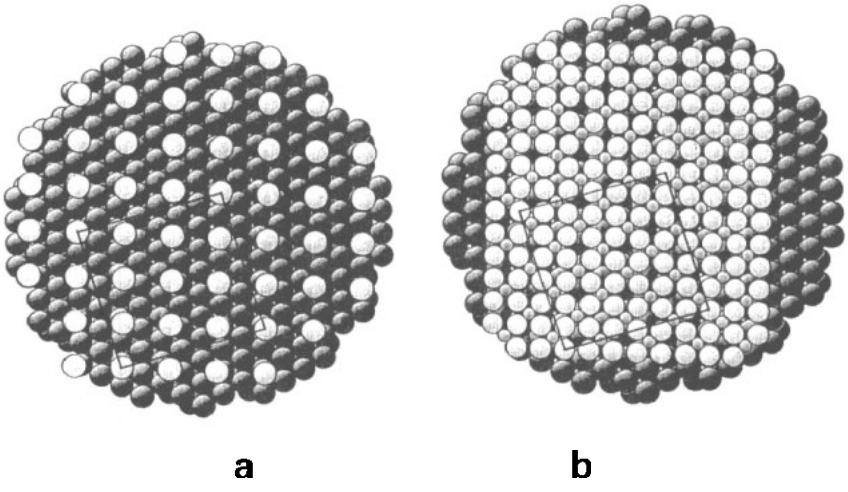

Figure 7. The top views of models of the Ni(111)c(5$\sqrt{3}$ × 9)rect.–C structure. (a) simply shows an Ni overlayer with one Ni atom per pseudo-(100)(2 × 2) mesh to establish the match of the periodicities. (b) shows the full structure. The larger shaded balls represent the Ni atoms and the smaller shaded balls represent the C atoms. The outermost reconstructed layer Ni atoms are shown lighter (and with a slightly reduced radius), and in (b) the overlayer is omitted on the edge for clarity. The primitive unit mesh is superimposed.

to expose apparent (0001) surfaces [93, 94], so the suggestion of multilayer reconstruction to the structure of another face is not unique.

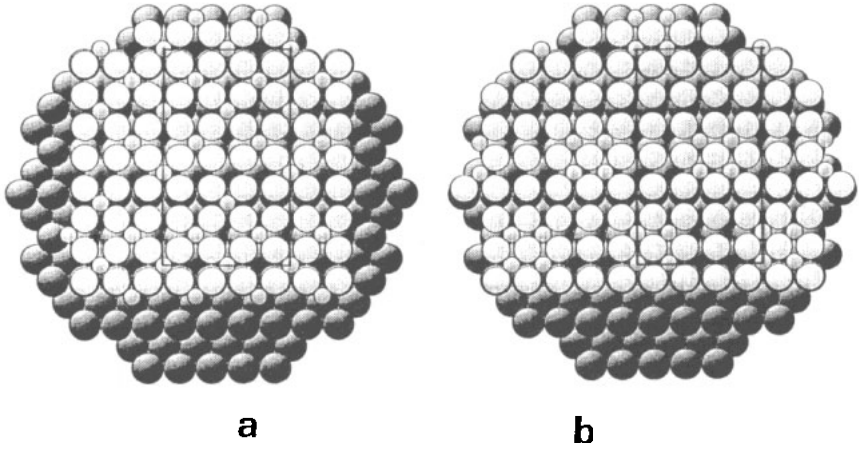

Figure 8. The top views of two possible models of the Ni(110)(4 × 5)–C structure both based on the same pseudo-(100) reconstruction. (a) simply shows a high- (0.6) ML) coverage C structure, which matches the basic symmetry requirements [98], while (b) is a lower-coverage modification, which could account for published STM images of this surface [101]. The larger shaded balls represent the Ni atoms and the smaller shaded balls represent the S atoms. The outermost reconstructed layer Ni atoms are shown lighter (and with a slightly reduced radius), and in (b) the overlayer is omitted from the lower edge for clarity. The unit mesh is superimposed.

One additional phase seen with N adsorption on Ni(100) is described as '(2×6)'–N. It has recently been suggested [11] that this is actually not a true commensurate phase, but rather $(2 \times L)$, although the apparent incommensurate character may be due to antiphase domain boundary effects; this phase is often found to coexist with the c($5\sqrt{3} \times 9$)rect.–N structure. It is proposed [11] that the (2×6) structure is a slight modification of the same pseudo-(100) reconstruction; in particular, while the $(5\sqrt{3} \times 2)$ phase involves a matching of ten (211)(111)-atom rows with eight (110)(100) rows of the pseudo-(100) overlayer, a commensurate (2×6) structure can be provided by a model in which six (211)(111)-atom rows of the substrate are matched by five (110)(100) rows of the overlayer. Notice that these matches lead to scope for 8% relaxation of the pseudo-(100) overlayer in the $(5\sqrt{3} \times 2)$ phase compared with only 4% for a commensurate (2×6) phase. The extra scope for relaxation may be especially important for the $(5\sqrt{3} \times 2)$–S reconstruction in view of the recently discovered large-amplitude 'clock' reconstruction of this overlayer [148], but may be less important for the C and N overlayers, for which 'clock' reconstructions can be accommodated even on the unrelaxed (100) face.

On Ni(110), the close similarity of the N and C adsorption phases is lost. In the case of C adsorption there appear to be two phases, (2×1) and (4×5) [95–100], having similar coverage and being prepared at slightly different temperatures, although the exact coverage seems to be in doubt and one intermediate value based on Auger electron spectroscopy [97] is used in table 4. The understanding of the structure of these two phases is currently very limited. Papagno *et al* [99] have proposed that local threefold-coordinated C adsorption sites are involved in the (2×1) phase, but this suggestion seems to be based more on speculation as to the likely nature of the local bonding than on actual experimental evidence from the angle-resolved valence-band photoemission they performed. Similarly, the recent study of the (4×5) phase by Paolucci *et al* [98] was also directed towards elucidation of the valence electronic structure, although these authors did note the systematic absence of certain LEED beams characteristic of a glide symmetry in the structure [101] (similar to that identified from the (100)(2×2)–C structure [75]). They proposed a structure that possesses the appropriate symmetry based on local distortions of the surface to (100)-like square clusters, but with no change in the outermost layer Ni atom density. The C coverage in their model is rather low (0.20 ML), and although the experimental determinations of the coverage are far from consistent, this value is much lower than the saturation coverages on the other faces. Recent STM images [100] also show the glide symmetry line along the surface (110) direction, and show asperities on an approximately square mesh, but with dark troughs along the surface (110) direction with the periodicity of the surface mesh. No structural interpretation has yet been offered by the authors of this paper.

Two possible models based on a pseudo-(100) reconstruction having the appropriate mesh and symmetry are shown in figure 8: the model in figure 8(a) has a coverage in this case of 0.6 ML (0.42 ML in (100) units), much more similar to the value on the other faces. This structure comprises two extra Ni atom rows (a total of seven) per unit mesh relative to the five rows of the (110) substrate, leading to an Ni–Ni periodicity parallel to the surface just 1% larger than that on the ideal (100) surface. The odd number of atom rows, however, can only match the pseudo-c(2×2) adsorbate periodicity by introducing a 'dislocation' across the centre of the unit mesh, which brings about the glide symmetry and slightly reduces the adsorbate coverage relative to the (100) surface structure. This saturation coverage is also reasonably close to the 0.5 ML implied by the (2×1) structure (for which one might reasonably assume a coverage of one C atom per unit mesh). The alternative model shown in figure 8(b) attempts to offer an explanation for the STM images by rearranging the C atoms on the pseudo-(100) overlayer into different hollow sites; the

particular model shown here has a lower C coverage of 0.4 ML, but the exact model needed to interpret the STM images actually depends considerably on the electronic structure and on the extent of any corrugation of the pseudo-(100) overlayer on the (110) substrate. The occupation of nearest-neighbour hollows in the model of figure 8(b) could also be expected to induce additional distortions.

The fact that the (2×1) structure is reported to lead to rather diffuse LEED patterns (and has not been seen in all studies), coupled with the fact that the (4×5) structure is produced at higher temperatures, both suggest that the (4×5) may be the more stable, lower-energy structure and that reconstruction, such as those suggested in figure 8, is probably involved.

While the structure of the Ni(110)–C structures is still in the realms of speculation, the situation for N adsorption on both Ni(110) and Cu(110) is significantly clearer. On both of these surfaces a single (2×3)–N phase is seen, presumably having the same basic structure on each surface. The first proposal as to the structure involved, for the Cu(110) surface, was supported by limited experimental studies using both low-energy ion scattering and photoelectron diffraction [102–104], and is shown in figure 9. This model involves one extra 'added row' of Cu atoms to a total of four to match the three rows per unit mesh of the underlying substrate. The overlayer then has a simple pseudo-(100)c(2×2) structure. This model has been disputed as a result of STM observations, in particular, which show regular troughs interpreted as being due to missing (rather than added) rows. Further low-energy ion-scattering measurements also appeared to lend support to this missing-row model [105, 106], while preliminary LEED results appeared to favour a quite different model having missing rows perpendicular to those 'seen' in STM [107]. A full quantitative surface x-ray-diffraction investigation, however, shows clearly that the added-row model of figure 9 is correct, but there is a considerable corrugation of the reconstructed layer perpendicular to the surface, which can account for the STM and ion-scattering results [108]. Recent further STM results [109] suggesting different structures at different N coverages would appear to be reconcilable with the same basic Cu surface reconstruction. Very recent high-energy ion-scattering results [110] provide further clear support for the added-row model of figure 9.

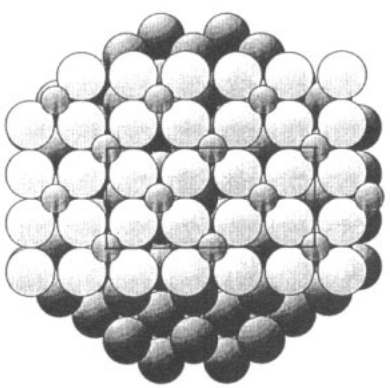

Figure 9. The top view of a model of the Cu(110)(2×3)–N (pseudo-(100)) structure. The larger shaded balls represent the Cu atoms and the smaller shaded balls represent the N atoms. The outermost reconstructed layer Cu atoms are shown lighter, and the overlayer is omitted on the edge for clarity. The unit mesh is superimposed.

The remaining structures formed by N adsorption on Cu surfaces are also summarized in table 4. Note that because Cu surfaces are generally unable to dissociate hydrocarbons or CO, there appears to be no literature on the adsorption phases that may be formed by C on Cu surfaces. One report [111] of the result of direct C deposition on (100) vicinals reported only graphitic structures, and while faceting did occur on heating, the surfaces still showed LEED patterns best described by a graphitic overlayer.

On the Cu(100) surface a simple c(2 × 2)–N phase is formed, and this has been analysed by LEED and shown to comprise the usual hollow-site adsorption structure, although the N atoms are very close to coplanar to the top Cu atom layer [112, 113]. Evidently this can be achieved on Cu(100) without the need for the reconstruction that occurs on Ni(100). On the other hand, recent STM images [114] suggest the situation may actually be slightly more complicated than this. In particular, these images show much of the surface covered with islands, which are interpreted as (100) Cu_2N structures with a Cu–Cu spacing actually 5% larger than that in the Cu(100) surface on which they lie. The size of the islands relates to the distance over which the nitride and metal surfaces are commensurate. The curious thing about this result is that the authors report a sharp c(2 × 2) LEED pattern, whereas the high surface coverage of the nitride (in the areas imaged by STM) would be expected to give far more complex LEED patterns, albeit with the strong features reasonably close to the half-order diffraction beams. One possibility is that the majority of the surface seen by LEED is a true c(2 × 2) structure, as investigated quantitatively by this technique [112, 113], and that the nitride islands are a more advanced state of nitridation, even, perhaps, involving more than one layer of the nitride structure.

On Cu(111), no quantitative structural studies of N adsorption have been made, but there is a report of an ordered structure seen in LEED [115], which appears to be incommensurate, but has been explained in terms of a slightly distorted square mesh of dimensions slightly larger than that of the (100)c(2 × 2) mesh: the implied Cu square mesh is 1.04 × 1.02 times larger than that on (100). The proposed interpretation is therefore of a pseudo-(100)c(2 × 2) reconstruction for this face, in common with that demonstrated for the (110) surface. The authors of this paper remark that this square-mesh Cu structure with coplanar N atoms that appears to form the basis of the surface structure of all three low-index faces of Cu is very similar to that of the (100) face of the bulk compound Cu_3Ni [116].

Although there appear to be no detailed studies of the γ-plot for any of these adsorption systems, one rather interesting observation of faceting does deserve comment. A study of the adsorption of N on Ni(210) [33] actually observed this surface, exposed at 77 K, to start to facet to (100) and (110) faces at temperatures as low as 148 K; the (110) surface is found to display the (2 × 3) phase discussed above, but the (100) face is reported to show a structure described as $(6\sqrt{2} \times \sqrt{2})R45°$. If we recall that the (100)c(2 × 2) phase is actually more correctly described as $(100)(\sqrt{2} \times \sqrt{2})R45°$, we see that this structure reported on the (100) facets appears to be a superstructure of the basic c(2 × 2) phase. Whether this larger periodicity relates to the constraints of preferred facet sizes, or to some other cause, is unknown. The result is interesting, however, in showing that the reconstructed (110)(2 × 3) phase clearly provides a local deep minimum in the γ-plot for this system.

In summary, therefore, we see that there is a significant body of evidence supporting the idea that most, if not all, of the most stable structures at high coverage produced by N and C adsorption phases formed on Cu and Ni surfaces involve reconstruction to square-submesh surface phases, basically having the c(2 × 2) structure of the (100) faces. Although, in the case of Cu–N, this structure is also closely related to that of a bulk compound, the situation is quite different from the Cu/S situation of the previous section in which different two-dimensional Cu–S structures are seen on each face, which correspond to different orientations of the bulk compound. Moreover, there is direct evidence that the (2 × 3)–N reconstruction on Ni(110) does, indeed, provide a low-surface-free-energy phase relative to any possible adsorption structures on nearby vicinal surfaces.

3.3. O adsorption on Cu surfaces

Finally, as an example of a rather different situation, we summarize the results of

experiments on the chemisorption of O on Cu surfaces. We chose this example partly because there was an early suggestion of a pseudo-(100) reconstruction of the (111) face in this system, but also because the results now highlight a rather different case of a bulk structural element appearing to dominate the behaviour. We do not consider O adsorption on Ni surfaces, because in this system thin multilayers of epitaxial bulk oxide start to form, even at room temperature and under low-vacuum conditions (although simple, small-unit-mesh, overlayer chemisorption phases also exist) [117]. By contrast, on Cu surfaces 'bulk' oxides can only be grown under more extreme conditions of temperature and pressure, and under typical UHV exposure conditions and at modest temperatures, only chemisorption structures are formed. This system is also of interest because it is one of the few for which there is a significant amount of published work concerning adsorbate-induced faceting under good vacuum conditions.

Table 5. Long-range-ordered structures formed by O adsorption on Cu surfaces.

	Phase		Coverage	
Surface	Wood	Matrix	(ML)	((100)-equivalent ML)
Cu(100)	$(2\sqrt{2} \times \sqrt{2})R45°$		0.50	0.50
Cu(111)	$c(8 \times 8)$	$\begin{vmatrix} 2 & 1 \\ -2 & 3 \end{vmatrix}$	0.49	0.57
Cu(110)	(2×1)		0.50	0.35
	$c(6 \times 2)$		0.67	0.47

Table 5 summarizes the long-range-ordered structures known to be produced on the three low-index faces of Cu due to O chemisorption structures. Good quantitative structural information is available for both the (100) and (110) surface structures, although the understanding of the (110)(2×1) phase came first. Specifically there is now a wealth of evidence from many techniques that this involves a 'missing-row' structure with alternate Cu atoms missing along the ⟨110⟩ close-packed rows, and the O atoms occupying the long-bridge sites (figure 10(a)) [118–123]. Strictly, we now know from STM studies of the formation of this structure [32, 124] that it is really an 'added-row' model, but the actual equilibrium structure is identical in either of these descriptions, and the missing-row description remains clearer. Although there has been some controversy concerning the exact O–Cu and Cu–Cu outermost layer spacings, it is clear that the O atoms lie quite close (< 0.3 Å) to coplanar with the outermost Cu atoms. The more complex (110)$c(6 \times 2)$–O phase, which requires much higher O exposures, has proved more difficult to solve (see, e.g., [125, 126]), but there is a rather detailed analysis, based particularly on surface x-ray diffraction, which indicates that the basic structural element of Cu–O–Cu chains is retained in the more substantial reconstruction [127]. In particular, while the (2×1) structure contains one ⟨100⟩ azimuth Cu–O–Cu chain per unit mesh (with two ⟨100⟩ Cu rows in the substrate in the same mesh), the $c(6 \times 2)$ contains two such overlayer chains per three substrate rows. Above these Cu–O–Cu chains, one additional Cu atom per primitive unit mesh (two for each $c(6 \times 2)$ unit) bridges pairs of adsorbed O atoms.

On the Cu(100) surface, the structure of chemisorbed O has proved to be a long-standing problem, although there is now rather clear convergence over most aspects of the structure (see [128] and references therein). For many years a $c(2 \times 2)$ phase was believed to exist at a coverage of 0.50 ML and was widely attributed to hollow-site adsorption with

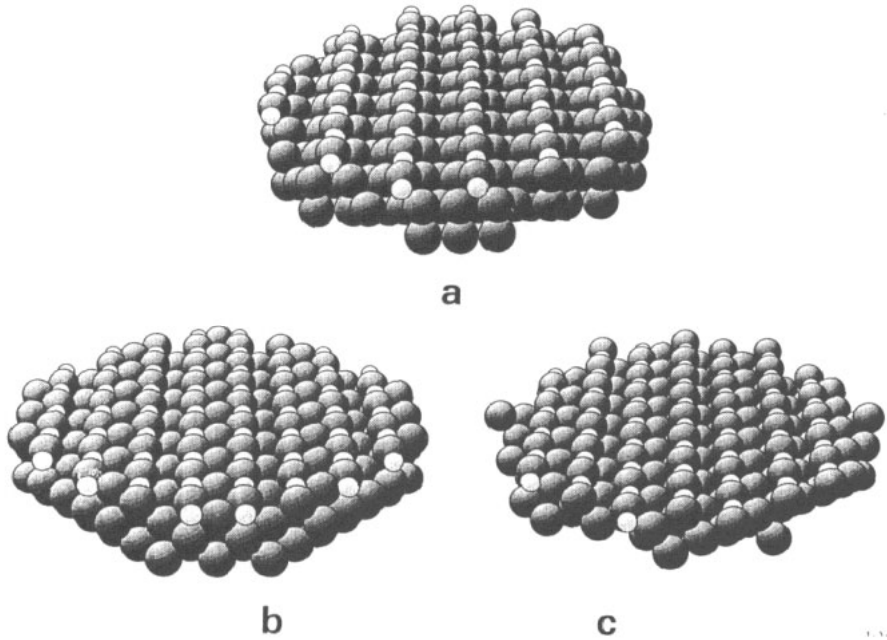

Figure 10. Perspective views of models of the (a) Cu(110)(2 × 1)–O, (b) Cu(100)(2$\sqrt{2}$ × $\sqrt{2}$)R45°–O and (c) Cu(410)–O structures, looking along the open ⟨100⟩ azimuth and the associated Cu–O–Cu chains. In each case the larger shaded balls represent the Cu atoms the smaller shaded balls represent the O atoms.

a Cu–O layer spacing of about 0.8 Å, very similar to the situation for O adsorption on Ni(100). There is now very serious doubt, however, as to whether such a phase exists [129], and while there is certainly a low-coverage phase at room temperature and below, the main stable chemisorption phase is recognised to be the (2$\sqrt{2}$ × $\sqrt{2}$)R45° structure, which corresponds to a coverage of 0.50 ML. Moreover, the main feature of this structure (figure 10(b)) [128, 130–135] is that, like the (110) surface, it involves missing Cu rows; in this case, only every fourth ⟨100⟩ row is missing, and the mechanism does indeed involve removal rather than addition of Cu atoms [133]. The O atoms in this structure adopt sites essentially coplanar with the outermost Cu layer, and occupy the sites that were fourfold-coordinated hollows prior to the row removal; they are thus nominally threefold coordinated, although the distance to the second-layer Cu atom below is similar, whereas some relaxation of atoms along the missing-row edge may occur, so the adsorbate atoms can be viewed as either twofold, threefold, or fourfold coordinated! The basic structure around the O adsorbates is, in any case, very similar to that on Cu(110), with essentially linear Cu–O–Cu–O chains being formed.

On the Cu(111) surface the situation is far less clear. Most studies (even those providing local structural information [136, 137]) report no long-range-ordered O induced phases on this surface, and only a loss of order is usually seen in LEED, although there are reports of ordered phases with complex LEED patterns and large-surface-mesh structures [138–142]. In particular, Judd *et al* [140] report a $\left|\begin{smallmatrix} 2 & 1 \\ -2 & 3 \end{smallmatrix}\right|$ LEED pattern, which they comment can be described in the Wood notation only by c(8 × 8) containing eight primitive unit meshes, for which the unit mesh is a slightly distorted version of a (100)(2$\sqrt{2}$ × 2$\sqrt{2}$)R45° structure.

On this basis they propose that the structure actually involves a pseudo-(100) reconstruction, presumably to the $(2\sqrt{2} \times \sqrt{2})$R45° structure, which requires two unit meshes to come into registry with the underlying (111) surface. This structure was produced by room-temperature exposure, although improved ordering was achieved by annealing to 100 °C. Although this model appears to fit our pattern of pseudo-(100) reconstructions on (111) surfaces, the fact that we now know that the Cu(100)$(2\sqrt{2} \times \sqrt{2})$R45°–O structure actually involves missing rows means that the plausibility of this simple interpretation seems more doubtful.

Recent STM studies of O adsorption on Cu(111), coupled with other techniques including high-energy ion scattering [141, 142] have identified two quite different complex structures having unit meshes given in the matrix notation by $\left|\begin{smallmatrix} 1 & 3 \\ -8 & 5 \end{smallmatrix}\right|$ and $\left|\begin{smallmatrix} 8 & 1 \\ -4 & 5 \end{smallmatrix}\right|$ (using the 60° included-angle substrate mesh as described earlier). Detailed models for these structures have been developed, both of which are proposed to be based on (111) sections through the bulk, slightly distorted structure of Cu_2O, but involving a total of five atomic layers. It is notable that these structures were prepared using exposure at 400 °C, and subsequent annealing at up to 500 °C, and it appears that they represent the earliest stages of 'bulk' oxide epitaxy (similar to the three-layer oxide structures seen on Ni). As such they probably fall outside our chosen area of concern in the present review.

The basic picture to emerge from O chemisorption studies of the three low-index surfaces of Cu is thus that a common structural element is certainly present on both (110) and (100) surfaces, namely the essentially linear Cu–O–Cu chains with a Cu–Cu spacing corresponding to that in a ⟨100⟩ direction in bulk Cu. The fact that this direction does not occur (and thus this spacing is not available) on the (111) surface offers a simple reason why simple ordered structures do not seem to form on this face. Moreover, the face that both Cu(110) and Cu(100) undergo Cu-atom-density-changing reconstructions on O adsorption indicates that these chemisorption structures are unlikely to form the basis of a reconstruction of the (111) surface.

Surface-energy studies [74] of the influence of O on Cu surfaces by the torque-term method actually find increasingly deep cusps in the γ-plot at the (100) and (111) surfaces, with the (111) cusp being deepest, but these measurements were conducted to 1000 °C, when, as we have already remarked above, the results may well be dominated by surface oxide epitaxy rather than simple chemisorption. However, even room temperature UHV studies show a tendency of some Cu surfaces to facet in the presence of O. In particular, (100) vicinals facet to (410) [111, 143, 144]. The special stability of the (410) under O exposure has attracted some attention. An early structural study using x-ray photoelectron diffraction [145] appears to identify the first O adsorption site on this surface as on the step edges to produce a local structure we now recognize as identical to that on the edge of missing rows in the Cu(100)$(2\sqrt{2} \times \sqrt{2})$R45°–O structure. In fact, the similarity of the terrace width on the (410) face and the size of the Cu(100)$(2\sqrt{2} \times \sqrt{2})$R45°–O unit mesh was remarked on in early studies of adsorption on the (410) face [111], and the apparent preference for O atoms to adopt the step-edge sites was one of the key ideas leading to the suggestion (prior to the availability of experimental evidence) that the Cu(100)$(2\sqrt{2} \times \sqrt{2})$R45°–O structure involved missing rows (see [128] and references therein). On the other hand, the fact that this (100) surface does produce such step-edge sites through its reconstruction argues against the need for faceting to achieve such sites. In fact recent STM studies [146] indicate that the (410) surface also has a missing row on the terraces in the presence of adsorbed O, producing a structure that effectively comprises step-edge sites (next to the missing row) and true isolated Cu–O–Cu chains like those on Cu(110) along the edges of the terraces (figure 10(c)). The evidence is therefore that even the faceting behaviour is determined by the strong preference for the special local chain geometry of the adsorbed O.

4. General discussion and conclusions

This survey of the sub-monolayer adsorption structures of S on Ni, Cu and Pt surfaces, N and C on Ni and Cu and O on Cu, has identified at least four distinct types of structure for which there appear to be reasonable quantitative structural evidence. There are as follows:

(i) In most cases, at least one, typically the lowest-coverage phase, comprises a simple commensurate overlayer with adsorption in the maximally coordinated site of the particular face being studied.

(ii) On the (111) faces most systems show strong evidence for one or more reconstructed phases at higher coverages, while there is evidence for similar behaviour on many of the (100) faces, but far fewer examples on (100) where a simple $c(2 \times 2)$ overlayer is generally the saturation phase. This is the class of adsorption structure that has attracted the greatest attention so far using quantitative methods.

(iii) With the exception of Cu/O, these reconstructions on the (111) and (110) faces fall into two categories:

(a) pseudo-(100) reconstructions having a local geometry similar to the overlayer phase on the (100) face (Ni/S, Ni/C, Ni/N, Cu/N) and

(b) structures associated with single or double layers of bulk compounds, the orientation and symmetry of the bulk compound layers matching those of the substrate (Cu/S).

(iv) The Cu/O case is a special one in that even the lowest-coverage well ordered structures on all three low-index faces reconstruct, and the key common element of the reconstructed phases is the incorporation of O into Cu–O–Cu chains with a periodicity equal to that of the ⟨100⟩ direction in Cu. The tendency for Cu to bond to pairs of O atoms is also a feature of bulk copper oxides (e.g. cuprate—Cu_2O [149]), and the Cu–O chains are a characteristic feature of the bulk structure of many of the cuprate 'ceramic' superconductors (see, for example, [150, 151] and references therein). Evidently the energetic preference for this almost one-dimensional structural element is carried over into the chemisorption structures.

In effect we therefore identify three different types of preferred stable structural element that form the reconstructed surfaces, which can be nominally described as two, three and one dimensional. In the pseudo-(100) reconstructions, the stable structure is sufficiently similar on several different orientations of substrate to imply that the bonding within this layer evidently dominates over considerations of energetic matching to the underlying substrate and we can loosely describe this as two dimensional. In the second category, a structure forms that is effectively a thin section of a (distorted) three-dimensional bulk-compound phase, but different sections form on different orientations of surface so the substrate epitaxy plays a key role. Finally, in the Cu–O case a common nominally one-dimensional structural element appears to dominate the stability of both surface and bulk-compound phases. Notice that the 'two-dimensional' structure may, as in the case of N on Cu, also correspond to a geometry very similar to that of a particular section through the associated bulk compound; one might deduce that this orientation of the compound represents a particularly low-surface-energy face to which faceting of the compound would occur, but there seems to be no evidence to support or refute this suggestion.

Within the full set of structural phases presented in tables 1–5 and discussed in the text there are, of course, many for which the detailed structure remains a matter of speculation, and in the most complex reconstructions there are real difficulties in finding techniques suitable for their complete solution. Nevertheless, there is sufficient evidence to support

the main points of the above summary, even if the generality of the conclusions remains unclear.

Because surface reconstructions (like any other structural phase) are determined by energy minimization, we have tried to collate some matching information on direct measurements of relative surface free energies, but such information is sparse. The clearest case seems to be the Pt/S case, for which equilibrium-shape measurements provide clear evidence that the (100) surface in the presence of the (2×2)–S and $c(2 \times 2)$–S phases has a deep cusp in the γ-plot. The implication of this result is that other low-index faces should probably facet in equilibrium. Unfortunately, the data on the S adsorption phases on Pt are sparse, but it appears that there may be no stable reconstructions on any of the faces. It may be, of course, that it is precisely the inability of the (111) and (110) faces to adopt structures similar to that on (100) which leads to the absence of these orientations on the equilibrium shape.

Of the other systems considered, the only clear and relevant information on the γ-plot originates from the observation that Ni(210) surfaces facet to (110) in the presence of adsorbed N, and that the facets show the Ni(110)(2×3)–N structure, which we are reasonably sure, by analogy with the same phase on Cu, does have a pseudo-(100) reconstruction. Here, at least, is clear evidence not only that the (100) chemisorption structure must have a very low energy to produce the (110) reconstruction, but also that the reconstructed face does provide a reasonably deep local cusp in the γ-plot. In this case, at least, the evidence is therefore also that the pseudo-(100) structure is stable rather than metastable.

Any attempt to understand these phenomena in greater depth needs input from both theory and experiment. There is no doubt that many of the structural phases discussed here, for which the structures proposed remain largely speculation, could be solved by further experiments. Even the large-unit-mesh structures may be tackled by surface x-ray diffraction. There is also considerable scope for further experiments on the role of adsorption under well defined conditions on the γ-plot; small-particle equilibration experiments are particularly attractive and while electron microscopy has already been shown to be effective in their study, STM holds great promise for similar studies. Answering the key question of whether a surface reconstruction is truly stable to possible faceting transitions is often not simple, however, because the high temperatures needed to ensure equilibrium is reached in a reasonable time may well lead to desorption or desegregation of an adsorbate. Here, theoretical work could prove crucial. Recent total-energy calculations of specific examples of both complex clean-surface reconstructions and adsorbate-induced reconstructions show that the methods are now available for such work (e.g. [1, 147]). Moreover, while such calculations would not, of course, separate out the interfacial strain energy in a pseudo-(100) reconstruction, some understanding of the separate components in the total energy can be obtained from calculations based on hypothetical substrate structures of varying periodicity. By a combination of such new experiments and calculations one might therefore expect to establish more clearly whether the trends discussed here are, indeed, a basis for understanding a range of adsorbate-induced surface reconstructions.

References

[1] King D A and Woodruff D P (ed) 1994 *The Chemical Physics of Solid Surfaces* vol 7 (Amsterdam: Elsevier)
[2] Somorjai G A and Van Hove M A 1989 *Prog. Surf. Sci.* **30** 201
[3] Dowben P A 1987 *CRC Crit. Rev. Solid. State Mater. Sci.* **13** 191
[4] Oed W, Starke U, Heinz K and Müller K 1991 *J. Phys.: Condens. Matter* **3** S223
[5] McCarroll J J, Edmonds T and Pitkethly R C 1969 *Nature* **223** 1260

[6] Edmonds T, McCarroll J J and Pitkethly R C 1971 *J. Vac. Sci. Technol.* **8** 68
[7] Warburton D R, Wincott P L, Thornton G, Quinn F M and Norman D 1989 *Surf. Sci* **211/212** 71
[8] Kitajima Y, Yokoyama T, Ohta T, Funabashi M, Kosugi N and Kuroda H 1989 *Surf. Sci.* **214** L261
[9] Ruan L, Stensgaard I, Besenbacker F and Laegsgaard E 1993 *Phys. Rev. Lett.* **71** 2963
[10] Woodruff D P 1994 *Phys. Rev. Lett.* **72** 2499
[11] Gardin D E, Batteas J D, Van Hove M A and Somorjai G A 1993 *Surf. Sci.* **296** 25
[12] Wulff G 1901 *Z. Kristallogr.* **34** 449
[13] see, e.g. Blakely J M 1973 *Introduction to the Properties of Crystal Surfaces* (Oxford: Pergamon)
[14] Mykura H 1966 *Solid Surfaces and Interfaces* (London: Routledge and Kegan Paul) p 25
[15] McLean M and Mykura H 1965 *Acta Metall.* **13** 1291
[16] Jefferson D A and Harris P J F 1988 *Nature* **332** 617
[17] Burton W K, Cabrera N and Frank F C 1951 *Phil. Trans. R. Soc.* A **243** 299
[18] Wang T, Lee C and Schmidt L D 1985 *Surf. Sci.* **163** 181
[19] Netzer F P and Kneringer G 1975 *Surf. Sci.* **51** 526
[20] Christmann K, Ertl G and Pignet T 1976 *Surf. Sci.* **54** 365
[21] A further complication in the temperature dependence of the γ-plot of clean Pt may be the different intrinsic reconstructions of, for example, the (100) face [22].
[22] Abernathy D L, Mochrie S G J, Zehner D M, Grübel G and Gibbs D 1992 *Phys. Rev.* B **45** 9272
[23] No quantitative structure analysis appears to have been made of the Pt(100)c(2 × 2)–S phase, but the translational symmetry excludes most reconstructions and the similar Ni(100)c(2 × 2)–S [4] and Pd(100)c(2 × 2)–S [24] structures are known to involve simple hollow site adsorption.
[24] Berndt W, Hora R and Scheffler M 1982 *Surf. Sci.* **117** 188
[25] Herring C 1951 *Phys. Rev.* **82** 87
[26] Hayek K, Glassl H, Gutmann A, Leonard H, Prutton M, Tear S P and Welton-Cook M R 1985 *Surf. Sci.* **152** 419
[27] Heegemann W, Meister K H, Bechtold E and Hayek K 1975 *Surf. Sci.* **49** 161
[28] Berthier Y, Perdereau M and Oudar J 1973 *Surf. Sci.* **36** 161
[29] Berthier Y, Perdereau M and Oudar J 1974 *Surf. Sci.* **44** 28
[30] Berthier Y, Oudar J and Huber M 1977 *Surf. Sci.* **65** 361
[31] Oudar J 1980 *Mater. Sci. Eng.* **42** 101
[32] Coulman D J, Wintterlin J, Behm R J and Ertl G 1990 *Phys. Rev. Lett.* **64** 1761
[33] Kirby R E, McKee C S and Roberts M W 1976 *Surf. Sci.* **55** 725
[34] Wood E A 1964 *J. Appl. Phys.* **35** 1306
[35] Park R L and Madden H H Jr 1968 *Surf. Sci.* **11** 188
[36] Rosenblatt D H, Tobin J G, Mason M G, Davis R F, Kevan S D, Shirley D A, Li C H and Tong S Y 1981 *Phys. Rev.* B **23** 3828
[37] Stöhr J, Jaeger R and Brennan S 1982 *Surf. Sci.* **117** 503
[38] Barton J J, Robey S W and Shirley D A 1986 *Phys. Rev.* B **34** 778
[39] Marcus P M, Demuth J E and Jepsen D W 1975 *Surf. Sci.* **53** 501
[40] Orders P J, Sinkovic B, Fadley C S, Trehan R, Hussain Z and Lecante J 1984 *Phys. Rev.* B **30** 1838
[41] Van Hove M A and Tong S Y 1975 *J. Vac. Sci. Technol.* **12** 230
[42] Demuth J E, Jepsen D W and Marcus P M 1974 *Phys. Rev. Lett.* **32** 1182
[43] Fauster E Th., Dürr H and Hartwig D 1986 *Surf. Sci.* **178** 657
[44] Ohta T, Kitajima Y, Stefan P M, Stefan M L, Kosingi N and Kuroda H 1986 *J. Physique Coll.* **47** C8 503
[45] van der Veen J F, Tromp R M, Smeenk R G and Saris F W 1979 *Surf. Sci.* **82** 408
[46] Baudoing R, Gauthier Y and Joly Y 1985 *J. Phys. C: Solid State Phys.* **18** 4061
[47] Gauthier Y, Aberdam D and Baudoing R 1978 *Surf. Sci.* **78** 339
[48] Warburton D R, Thornton G, Norman D, Richardson C H, McGrath R and Sette F 1987 *Surf. Sci.* **189/190** 495
[49] Perdereau M and Oudar J 1970 *Surf. Sci.* **20** 80
[50] Besenbacher F, Stensgaard I, Ruan L, Norskov J K and Jacobsen K W 1992 *Surf. Sci.* **272** 334
[51] Besenbacher F and Stensgaard I 1994 *The Chemical Physics of Solid Surfaces* vol 7, ed D A King and D P Woodruff (Amsterdam: Elsevier)
[52] Ruan L, Stensgaard I, Laegsgaard E and Besenbacker F 1993 *Surf. Sci.* **296** 275
[53] Foss M, Fiedenhans'l R, Nielsen M, Findeisen E, Buslaps T, Johnson R L, Besenbacher F and Stensgaard I 1993 *Surf. Sci.* **296** 283
[54] Steinbrunn A, Dumas P and Colson J C 1978 *Surf. Sci.* **74** 201
[55] Muryn C A, Purdie D, Hardman P, Johnson A L, Prakash N S, Raiker G N and Thornton G 1990 *Faraday Discuss. Chem. Soc.* **89** 77

[56] Domange J L and Oudar J 1968 *Surf. Sci.* **11** 124
[57] Barton J J, Bahr C C, Hussain Z, Robey S W, Tobin J G, Klebenoff L E and Shirley D A 1983 *Phys. Rev. Lett.* **51** 272
[58] Bullock E L, Fadley C S and Orders P J 1983 *Phys. Rev.* B **28** 4837
[59] Zeng H C, Sodhi R N S and Mitchell K A R 1986 *Surf. Sci.* **177** 329
[60] Zeng H C, McFarlane R A and Mitchell K A R 1989 *Phys. Rev.* B **39** 8000
[61] Bahr C C, Barton J J, Hussain Z, Robey S W, Tobin J G and Shirley D A 1987 *Phys. Rev.* B **35** 3773
[62] Wu Z Q, Xu M L, Chen Y, Tong S Y, Mohmed M H and Kesmodel L L 1987 *Phys. Rev.* B **36** 9329
[63] Patel J R, Berreman D W, Sette F, Citrin P H, Rowe J E, Cowan P L, Jach T and Karlin B 1989 *Phys. Rev.* B **40** 1330
[64] Vlieg E, Robinson I K and McGrath R 1990 *Phys. Rev.* B **41** 7896
[65] Jiang Q T, Fenter P and Gustafsson T 1990 *Phys. Rev.* B **42** 9291
[66] Zeng H C, McFarlane R A and Mitchell K A R 1990 *Can. J. Phys.* **68** 353
[67] Schach von Wittenau A E, Hussain Z, Wang L Q, Huang Z Q, Li Z G and Shirley D A 1992 *Phys. Rev.* B **45** 13 614
[68] Campbell C T and Koel B E 1987 *Surf. Sci.* **183** 100
[69] Prince N P, Seymour D L, Ashwin M J, McConville C F, Woodruff D P and Jones R G 1990 *Surf. Sci.* **230** 13
[70] Ruan L, Stensgaard I, Besenbacher F and Laegsgaard E 1992 *Ultramicroscopy* **42–44** 498
[71] Atrei A, Johnson A L and King D A 1991 *Surf. Sci.* **254** 65
[72] Stensgaard I, Ruan L, Besenbacher F, Jensen F and Laegsgaard E 1992 *Surf. Sci.* **269/270** 81
[73] Boulliard J C and Sotto M P 1989 *Surf. Sci.* **217** 38
[74] Mykura H 1968 *Monograph 28, Surface Phenomena of Metals* (London: Society of Chemists in Industry) p 163
[75] Onuferko J H, Woodruff D P and Holland B W 1979 *Surf. Sci.* **87** 357
[76] Daum W, Lehwald S and Ibach H 1986 *Surf. Sci.* **178** 528
[77] Rahman T S and Ibach H 1985 *Phys. Rev. Lett.* **54** 1933
[78] Rocca M, Lehwald S, Ibach H and Rahman T S 1987 *Phys. Rev.* B **35** 9510
[79] Müller J E, Wuttig M and Ibach H 1986 *Phys. Rev. Lett.* **56** 1583
[80] Reindl S, Aligia A A and Bennemann K H 1988 *Surf. Sci.* **206** 20
[81] Sander D, Linke U and Ibach H 1992 *Surf. Sci.* **272** 318
[82] Woodruff D P 1994 *The Chemical Physics of Solid Surfaces* vol 7, ed D A King and D P Woodruff (Amsterdam: Elsevier)
[83] McConville C F, Woodruff D P, Kevan S D, Weinert M and Davenport J W 1986 *Phys. Rev.* B **34** 2199
[84] Kilcoyne A L D, Woodruff D P, Rowe J E and Gaylord R H 1989 *Phys Rev.* B **34** 12 604
[85] Hayden A B, Pervan P and Woodruff D P 1994 *Surf. Sci.* **306** 99
[86] Bader M, Ocal C, Hillert B, Haase J and Bradshaw A M 1987 *Phys. Rev.* B **35** 5900
[87] Kilcoyne A L D, Woodruff D P, Robinson A W, Lindner Th, Somers J S and Bradshaw A M 1991 *Surf. Sci.* **253** 107
[88] Gauthier Y, Baudoing-Savois R, Heinz K and Landskron H 1991 *Surf. Sci.* **251/252** 493
[89] Arvanitis D, Baberschke K and Wenzel L 1988 *Phys. Rev.* B **37** 7143
[90] Wenzel L, Arvanitis D, Daum W, Rotermund H H, Stöhr J, Baberschke K and Ibach H 1987 *Phys. Rev.* B **36** 7689
[91] Conrad H, Ertl G, Küppers J and Latta E E 1975 *Surf. Sci.* **50** 296
[92] Hemminger J C, Mutterties E L and Somorjai G A 1979 *J. Am. Chem. Soc.* **101** 117
[93] Barrett S D 1992 *Surf. Sci. Rep.* **14** 271
[94] Blyth R I R, Cosso R , Dhesi S S, Newstead K, Begley A M, Jordan R G and Barrett S D 1991 *Surf. Sci.* **251/252** 722
[95] Pitkethly R C 1970 *Chemisorption and Catalysis* ed P Hepple (London: Institute of Petroleum)
[96] Ertl G 1969 *Molecular Processes at Solid Surface* ed E Drauglis, R D Gretz and R I Jaffee (New York: McGraw-Hill)
[97] McCarty J G and Madix R J 1975 *J. Catal.* **38** 402
[98] Paolucci G, Rosei R, Prince K C and Bradshaw A M 1985 *Appl. Surf. Sci.* **22/23** 582
[99] Papagno L, Conti M, Caputi L S, Anderson J and Lapeyre G J 1991 *Phys. Rev.* B **44** 1904
[100] Klink C, Besenbacher F, Stensgaard I and Laegsgard E, to be published (as cited in [51])
[101] Holland B W and Woodruff D P 1973 *Surf. Sci.* 36 488
[102] Ashwin M J and Woodruff D P 1990 *Surf. Sci.* **237** 108
[103] Robinson A W, Woodruff D P, Somers J S, Kilcoyne A L D, Ricken D E and Bradshaw A M 1990 *Surf. Sci.* **237** 99

[104] Ashwin M J, Woodruff D P, Kilcoyne A L D, Robinson A W, Somers J S, Ricken D E and Bradshaw A M 1991 *J. Vac. Sci. Technol.* A **9** 1856
[105] Niehus H, Spitzl R, Besocke K and Comsa G 1991 *Phys. Rev.* B **43** 12619
[106] Spitzl R, Niehus H and Comsa G 1991 *Surf. Sci.* **250** L355
[107] Grimsby D T, Zhou M Y and Mitchell K A R 1992 *Surf. Sci.* **271** 519
[108] Baddorf A P, Zehner D M, Helgesen G, Gibbs D, Sandy A R and Mochrie S G J 1993 *Phys. Rev.* B **48** 9013
[109] Leibsle F M, Davis R and Robinson A W 1993 *Phys. Rev.* B **47** 10052
[110] Dürr H, Poker D B, Zehner D M and Barrett J H *Phys. Rev. Lett.* submitted
[111] Perdereau J and Rhead G E 1971 *Surf. Sci.* **24** 555
[112] Zheng H C, Sodhi R N S and Mitchell K A R 1987 *Surf. Sci.* **188** 599
[113] Zeng H C and Mitchell K A R 1989 *Langmuir* **5** 829
[114] Leibsle F M, Flipse C F J and Robinson A W 1993 *Phys. Rev.* B **47** 15865
[115] Higgs V, Hollins P, Pemble M E and Pritchard J 1986 *J. Electron. Spectrosc. Relat. Phenom.* **39** 137
[116] Wyckoff R W G 1960 *Crystal Structures* vol II (New York: Interscience) p V-15
[117] See, e.g., Brundle C R and Broughton J Q 1990 *The Chemical Physics of Solid Surfaces and Heterogeneous Catalysis* vol 3A, ed D A King and D P Woodruff (Amsterdam: Elsevier) p 131
[118] Bader M, Puschmann A, Ocal C and Haase J 1986 *Phys. Rev. Lett.* **57** 3273
[119] Yarmoff J A, Cyr D M, Huang J H, Kim S and Williams R S 1986 *Phys. Rev.* B **33** 3856
[120] Robinson A W, Somers J S, Ricken D E, Bradshaw A M, Kilcoyne A L D and Woodruff D P 1990 *Surf. Sci.* **227** 237
[121] Feidenhans'l R, Grey F, Johnson R L, Mochrie S G J, Bohr J and Nielsen M 1990 *Phys. Rev.* B **41** 5420
[122] Parkin S R, Zeng H C, Zhou M Y and Mitchell K A R 1990 *Phys. Rev.* B **41** 5432
[123] Dürr H, Fauster Th and Schneider R 1991 *Surf. Sci.* **244** 237
[124] Jensen F, Besenbacher F, Laegsgaard E and Stensgaard I 1990 *Phys. Rev.* B **41** 10233
[125] Hillert B, Becker L, Pedio M and Haase J 1990 *Europhys. Lett.* **12** 247
[126] Coulman D J, Wintterlin J, Barth J V, Ertl G and Behm R J 1990 *Surf. Sci.* **240** 151
[127] Fiedenhans'l R, Grey F, Nielsen M, Besenbacher F, Jensen F, Laegsgaard E, Stensgaard I, Jacobsen K W, Norskov J K and Johnson R L 1990 *Phys. Rev. Lett.* **65** 2027
[128] Asensio M C, Ashwin M J, Kilcoyne A L D, Woodruff D P, Robinson A W, Lindner Th, Somers J S, Ricken D E and Bradshaw A M 1991 *Surf. Sci.* **236** 1
[129] Mayer R, Zhang C S and Lynn K G 1986 *Phys. Rev.* B **33** 8899
[130] Zeng H C, McFarlane R A and Mitchell K A R 1989 *Surf. Sci.* **208** L7
[131] Wöll Ch, Wilson R J, Chiang S, Zeng H C and Mitchell K A R 1990 *Phys. Rev.* B **42** 11926
[132] Robinson I K, Vlieg E and Ferrer S 1990 *Phys. Rev.* B **42** 6954
[133] Jensen F, Besenbacher F, Laegsgaard E and Stensgaard I 1990 *Phys. Rev.* B **42** 9206
[134] Zeng H C and Mitchell K A R 1990 *Surf. Sci.* **239** L571
[135] Atrei A, Bardi U, Rovida G, Zanazzi E and Casalone G 1990 *Vacuum* **41** 333
[136] Niehus H 1983 *Surf. Sci.* **130** 41
[137] Haase J and Kuhr H-J 1988 *Surf. Sci.* **203** L695
[138] Ertl G 1967 *Surf. Sci.* **6** 208
[139] Simmons G W, Mitchell D F and Lawless K R 1967 *Surf. Sci.* **8** 130
[140] Judd R W, Hollins P and Pritchard J 1986 *Surf. Sci.* **171** 643
[141] Jensen F, Besenbacher F, Laegsgaard E and Stensgaard I 1991 *Surf. Sci.* **259** L774
[142] Jensen F, Besenbacher F and Stensgaard I 1992 *Surf. Sci* **269/270** 400
[143] Berndt W 1967 *Z. Naturf.* **22** 1655
[144] Sotto M 1992 *Surf. Sci.* **260** 235
[145] Thompson K A and Fadley C S 1984 *Surf. Sci.* **146** 261
[146] Lloyd G W W and Woodruff D P 1993 *Surf. Sci.* **283** L503
[147] Besenbacher F and Norskov J K 1993 *Prog. Surf. Sci.* **44** 5
[148] Foss M, Feidenhans'l R, Nielsen M, Findeisen E, Johnson R L, Buslaps T, Stensgaard I and Besenbacher F to be published
[149] Wyckoff R W G 1965 *Crystal Structures* vol 2 (New York: Interscience)
[150] Yvon K and François M 1989 *Z. Phys.* B **76** 413
[151] Sequeira A 1991 *Physica* B **174** 311